Applied Energy 135 (2014) 43–52

Contents lists available at ScienceDirect

Applied Energy

journal homepage: www.elsevier.com/locate/apenergy

Sensitivity of the CO_2 storage capacity of underground geological structures to the presence of SO_2 and other impurities

Zaman Ziabakhsh-Ganji *, Henk Kooi

Critical Zone Hydrology Group, Department of Earth Sciences, VU University Amsterdam, De Boelelaan 1085, 1081 HV, Amsterdam, The Netherlands

HIGHLIGHTS

- Impure CO_2 can both enhance and suppress storage capacity.
- The storage capacity depends on the gas species and *P–T* conditions.
- Co-injection of SO_2 appears a viable method to enhance storage capacity.

ARTICLE INFO

Article history:
Received 16 May 2014
Received in revised form 10 August 2014
Accepted 18 August 2014

Keywords:
Carbon capture storage
Storage capacity
Impurity
Solubility
Sulfur dioxide (SO_2)

ABSTRACT

Depleted hydrocarbon reservoirs and deep saline aquifers are key targets for geological storage of CO_2 to reduce atmospheric CO_2 emissions. Most studies in CCS investigate subsurface storage of pure CO_2. In this paper we investigate the impact of the presence of other gases (impurities) in the injected CO_2 stream on solubility trapping (in the aqueous phase) and volumetric trapping (in the non-aqueous phase, for a wide range of pressure and temperature. Calculations for solubility trapping are based on an equation of state that accurately accounts for the pressure, temperature, gas-compositional (mixtures) and salinity influences on CO_2 solubility and brine density. For volumetric trapping the Peng–Robinson equation of state is used, accounting for binary interaction for gas mixtures and density correction. In the analysis, special attention is paid to the impact of SO_2, which exhibits anomalous storage effects when compared to other common impurities.

It is shown that while most impurities reduce the CO_2 storage capacity (STC) in both the aqueous and non-aqueous phase, presence of SO_2 enhances STC in both phases for a wide range of pressure and temperature conditions. However, for the realistic amounts of SO_2 in flue gases, the effects are rather small; for a SO_2 content of about 0.5% the non-aqueous STC enhancement ranges up to about 4%.

For volumetric trapping, the greatest positive impact of SO_2 occurs at relatively low pressures (74–100 bar) and temperatures (313–325 K). These are typical for shallow (<1 km) aquifers or deeper depleted hydrocarbon reservoirs during the injection stage. For solubility trapping, the STC enhancement by SO_2 increases with pressure and is relatively insensitive to temperature, implying that the greatest positive effect would be achieved for deep saline aquifers. These findings suggest that the positive effects of SO_2 on the CO_2 storage capacity could be of practical significance for CCS projects. The positive storage effects would have to be evaluated relative to possible negative effects due to induced geochemical reactions, corrosion of well casings, and health risks associated with potential leakage from transport or injection facilities or from the storage reservoir.

1. Introduction

Storage of CO_2 in underground geological structures is considered an important methodology to reduce, and ultimately reverse, the trend of increasing carbon dioxide (CO_2) concentrations in the atmosphere [1]. Carbon dioxide capture and storage (CCS) generally involves capture of CO_2 at major stationary sources such as power plants and injection in underground geological structures such as saline aquifers, depleted hydrocarbon reservoirs, or producing hydrocarbon reservoirs to enhance oil or gas recovery. In general, captured CO_2 contains additional gases – these are commonly referred to as co-contaminant gases or impurities – such as H_2S, CH_4, SO_2, N_2 and O_2. The first two impurities (H_2S, CH_4) are

* Corresponding author. Tel.: +31 20 5987264; fax: +31 20 5989940.
E-mail address: z.ziabakhshganji@vu.nl (Z. Ziabakhsh-Ganji).

http://dx.doi.org/10.1016/j.apenergy.2014.08.073
0306-2619/

Nomenclature

a	energy parameter for PR EOS
A	dimensionless energy parameter
b	volume parameter of PR EOS
B	dimensionless volume parameter
k_{ij}	binary interaction coefficient
P	pressure (bar)
T	temperature (K)
R	universal gas constant 83.1447 cm^3 bar K^{-1} mol^{-1}
Z	compressibility factor
M	molality (mol kg^{-1} H_2O)
T_c	critical temperature (K)
P_c	critical pressure (bar)
VLE	vapour liquid equilibrium
STC	storage capacity
STCV	volumetric storage trapping capacity
STCS	solubility storage trapping capacity
S_{wr}	residual water saturation
c	correction factor (cm^3 mol^{-1})

Greek symbols

ω	acentric factor
χ	adjustable parameter in density correction
ρ	density (kg/m^3)
δ	bulk modulus
γ	constant coefficient

Subscripts

AqP	aqueous phase
NaqP	non-aqueous phase
s	mass of dissolved CO_2
mix	mixture
Res	reservoir

common in acid gas that is produced in hydrocarbon production units. The other gases are common components of flue gas captured at power plants [2,3].

Evaluating the CO_2 storage capacity of underground storage structures is rather involved. Injected CO_2 is generally trapped in different forms: (a) as a separate gas phase or supercritical fluid (called static, residual or volumetric gas trapping), (b) in an aqueous phase, often brines (solubility trapping), and (c) as a solid phase (mineral trapping) [4]. Moreover, the storage capacity of individual structures also depends on the reservoir geometry, its porosity structure and ambient pressure and temperature conditions [5].

Several methods exist for the quantification of storage capacity. Some methods for hydrocarbon reservoirs use production parameters such as the oil/gas recovery factor and the original gas/oil in place [5] to estimate how much CO_2 can be stored. Tseng et al. [6] developed an analytical method to account for the influence of water drive in gas reservoirs on CO_2 storage capacity. Zhou et al. [7] presented an approach to assess the storage capacity for saline aquifers. Denga et al. [8] considered the impact of geologic heterogeneity on CO_2 storage capacity. While all these studies considered storage of pure CO_2, capabilities to investigate presence and impacts of other (gaseous) components than CO_2 on the CO_2 storage capacity are still limited. Evaluation of the impacts of the presence of such components is important because they modify fluid properties (e.g. density) of the gas/liquid streams. Moreover, knowledge of the consequences of impurities in the CO_2 stream is of particular interest as high-level purification of CO_2 is costly and injection of co-contaminants with the CO_2 may therefore reduce the front-end processing costs of CCS. These costs of purification of CO_2 are estimated represent about ¾ of the total costs of CCS [9].

In this paper, we explore the impacts of impurities on both volumetric trapping and solubility trapping of CO_2 in underground storage reservoirs. For volumetric storage trapping, Wang et al. [10] have recently evaluated the impact of co-contaminants which predominate in oxyfuel flue gas, notably N_2, O_2 and Ar by using the Peng–Robinson equation of state (PR-EOS). Rather than studying specific storage reservoirs and their geometries, these authors focused on the P, T-influences on the density of supercritical gas mixtures (CO_2 trapping for the gas-available pore space). Wang et al. [10] showed that the reduction of the storage capacity of CO_2 due to the presence of the studied impurities is greater than the volume fractions of the impurities in the mixture. Therefore, the impurities are rather detrimental for the storage capacity of CO_2. However, in a prior report, Wang et al. [11] showed that SO_2 exhibits opposite behavior, and can enhance the volumetric storage capacity. They showed that at 330 K and for 2.9% SO_2, the CO_2 storage capacity can be up to 5% higher than for pure CO_2 storage, and that the maximum storage capacity occurs at about 11 MPa. In this paper, we expand on this finding and demonstrate the impact of SO_2 on storage capacity for a more extensive range of temperature and pressure conditions that can occur at CCS sites, and for different amounts of SO_2. Moreover, we use density corrections to the PR-EOS to achieve higher model accuracy. To our knowledge the impact of impurities on solubility trapping has not been analyzed before. Our approach uses our recently developed equation of state for gas mixtures and brine [12] in combination with a model for aqueous phase density calculation.

The paper is organized as follows. First, we elucidate the storage capacity estimation method for both volumetric and solubility trapping. Then, the results of sensitivity analyses are presented which illustrate the impact of the various gases, and in particular SO_2, on CO_2 storage.

2. Method

2.1. Volumetric storage trapping capacity (STCV)

For any given storage reservoir, the total mass of CO_2 that can be stored in the form of a separate gas phase or supercritical fluid depends on the pore space that is available for this form of storage. For storage of pure CO_2 for instance, Bachu et al. [5] proposed that the total CO_2 mass can be estimated using

$$M_{CO_2} = \rho_{CO_2} V_{Res}\ \phi(1 - S_{wr}) \tag{1}$$

where ρ_{CO_2} is the (dry) CO_2 density, V_{Res} is the total reservoir volume, and ϕ and S_{wr} are the reservoir-averaged porosity and the (irreducible) water saturation, respectively. In our approach we use this conceptual model and assume that storage of impure CO_2 does not change the available space for the non-aqueous phase storage. The method therefore does not account for mineral dissolution and precipitation processes that tend to accompany the storage of these gases. With these assumptions, for impure CO_2 storage the total mass of CO_2 stored is given by

$$M = \frac{\rho_{mix}}{1 + \sum_i \frac{m_i}{m_{CO_2}}} V_{Res} \phi (1 - S_{wr}) \tag{2}$$

where ρ_{mix} is the density of the gas mixture and m_i/m_{CO_2} is the ratio of the mass of impurity i to the mass of CO_2 in the mixture.

The ratio of Eqs. (2) and (1) now yields an intelligible measure to quantify the impact of impurities on volumetric CO_2 storage:

$$\mathrm{STCV} = \frac{M}{M_{CO_2}} = \frac{\rho_{mix}}{\rho_{CO_2}\left(1 + \sum_i \frac{m_i}{m_{CO_2}}\right)} \tag{3}$$

When STCV < 1 the impurities reduce the CO_2 storage capacity and vice versa for STCV > 1. The normalized volumetric CO_2 storage capacity STCV is identical to the quantity STC used by Wang et al. [10]. Our approach differs from Wang et al. [10] in that we use slightly more accurate density calculations and consider additional/other gas species. For the calculation of densities, we use the Peng Robinson Equation of State (PR-EOS) [13]. However, it is well known that the PR-EOS, as well as other classical EOS's, provide a good fit of the vapour pressure for most substances, but that the prediction of molar volume and, hence, density, are rather poor. Therefore, we apply a correction method proposed by Mathias et al. [14], which is an extension of the simpler 'volume-shift method' of Peneloux et al. [15]. Hence, the density of the gas mixture is calculated using

$$\rho = \frac{Mw}{V^{PR} + c} \tag{4}$$

where Mw is the molecular weight, V^{PR} is the molar volume, and c is a correction factor or volume shift. The correction factor [14] is

$$c = \chi + f_c\left(\frac{0.41}{0.41 + \delta}\right), \quad \delta = -\frac{(V^{PR})^2}{RT}\left(\frac{\partial P}{\partial V^{PR}}\right)_T \tag{5}$$

where χ is a parameter which is constant for a gas species and which is obtained by regression of density data; δ, is the bulk modulus, and f_c is given by

$$f_c = V_c - (3.946b + \chi) \tag{6}$$

In Eq. (6), b is the co-volume and V_c is the molar volume in the critical point.

In our model the molar volume ($V^{PR} = ZRT/P$) is calculated directly from the PR-EOS. The compressibility factor, Z, obeys

$$Z^3 - (1 - B)Z^2 + (A - 2B - 3B^2)Z - (AB - B^2 - B^3) = 0 \tag{7}$$

Parameters A and B are a function of pressure and temperature and are defined as follows

$$A = \frac{a(T)P}{(\mathrm{RT})^2}, \quad B = \frac{bP}{\mathrm{RT}} \tag{8}$$

where

$$a(T) = 0.45724 \times \frac{R^2T_c^2}{P_c}\left[1 + (0.37464 + 1.54226\omega - 0.26992\omega^2)\left(1 - \sqrt{\frac{T}{T_c}}\right)\right]^2 \tag{9}$$

and

$$b = 0.07780\frac{RT_c}{P_c} \tag{10}$$

where ω, T_c, P_c and R are the acentric factor, critical temperature, critical pressure and gas constant respectively. For gas mixtures, we use standard simple mixing rules and binary interaction coefficients [16]

$$a_{mix}(T) = \sum_{i=1}\sum_{j=1} x_i x_j \sqrt{a_i(T)a_j(T)}(1 - k_{ij}), \quad b_{mix} = \sum_{i=1}^{n} x_i b_i \tag{11}$$

where x is the mole fraction of each component in the mixture. Table 1 lists the values of the binary interaction coefficients (k_{ij}) that were used. Most values were adopted from Li and Yan [17]. The listed value for CO_2–SO_2 was optimized using vapour liquid equilibrium experimental data from Cummings [18], results of which will be shown in the results section.

Table 1
Binary interaction coefficient values for the PR EOS (k_{ij}).

Gas	CH_4	H_2S	O_2	N_2	SO_2	Ar
CO_2	0.1	0.099	0.114	0.07	0.047	0.163

When Eq. (7) has three roots, to obtain the proper value of Z in $V^{PR} = ZRT/P$, we follow the approach described by Danesh [19]. In this case the intermediate one is ignored and the root yielding the lowest Gibbs free energy between the remaining two is selected. Let Z_h and Z_l be the two real roots with $\frac{G_h}{\mathrm{RT}}$ and $\frac{G_l}{\mathrm{RT}}$ being the Gibbs free energy, and where the subscripts denote the high and low Z value respectively. The difference in Gibbs free energy is given by:

$$\frac{(G_h - G_l)}{\mathrm{RT}} = (Z_h - Z_l) + \ln\left(\frac{Z_l - B}{Z_h - B}\right) - \frac{A}{B(\gamma_2 - \gamma_1)} \times \ln\left[\left(\frac{Z_l + \gamma_1 B}{Z_l + \gamma_2 B}\right)\left(\frac{Z_h + \gamma_2 B}{Z_h + \gamma_1 B}\right)\right] \tag{12}$$

where γ_1 and γ_2 for the PR-EOS are $1 + \sqrt{2}$ and $1 - \sqrt{2}$ respectively. If $\frac{(G_h - G_l)}{\mathrm{RT}}$ in Eq. (12) is positive Z_l is selected; otherwise Z_h is the correct root.

Following Mathias et al. [14], for mixtures the quantities V^{PR} and δ are determined by the mixing rule chosen for the PR-EOS (here Eq. (11)) while the correction factor for the mixture, c_{mix}, is obtained using

$$\chi_{mix} = \sum_{i=1}^{n} x_i\chi_i, \quad V_{c,mix} = \sum_{i=1}^{n} x_i V_{ci}, \quad Mw_{mix} = \sum_{i=1}^{n} x_i Mw_i \tag{13}$$

where x_i is the mole fraction of each component in the mixture. The molecular weight for the mixture is similarly averaged. Combining the above relationships yields the following expression for the storage capacity.

$$\mathrm{STCV}(P,T) = \frac{\left(\frac{Mw}{V^{PR}+c}\right)_{mix}}{\left(\frac{Mw}{V^{PR}+c}\right)_{CO_2}\left(1 + \sum_i \frac{x_i Mw_i}{x_{CO_2} Mw_{CO_2}}\right)} \tag{14}$$

The values of χ_i for the pure gas species in this study, and for temperatures ranging from 1 to 170 °C and pressures up to 700 bar, are listed in Table 2. The values were obtained using the Weighted Nonlinear Least Squares (WNLS) method [20] and density data from the NISTa [21] database (http://webbook.nist.gov/chemistry/fluid/).

2.2. Solubility storage trapping capacity (STCS)

As mentioned by Bachu et al. [5] solubility trapping is a continuous, time-dependent process which, in particular for saline aquifers, tends to become more effective over longer time scales. The ultimate storage (capacity) of a finite size reservoir is reached when all the water in the reservoir has reached solubility saturation. Therefore, analogous to Eq. (1) for volumetric storage, the mass of CO_2 that can be stored by solubility trapping can be determined using [5,22]:

$$M_{s_{CO_2}} = V_{Res}\ \phi S_{wr}\left(\rho_{AqP} X_{CO_2} - \rho^0_{AqP} X^0_{CO_2}\right) \tag{15}$$

Table 2
Density correction parameter values for the PR EOS.

Gas	CO_2	CH_4	H_2S	O_2	N_2	SO_2	Ar
χ	3.3894	6.4044	3.939	5.1749	6.8527	1.4431	5.2851

where ρ_{AqP} is the density of formation water, X_{CO_2} is the carbon dioxide content (mass fraction) in formation water and the superscript 0 refers to the initial carbon dioxide content of the formation brine. Here, for simplicity we assume that initial carbon dioxide content is negligible. This seems very reasonable as our calculations for an initial partial CO_2 pressure of 4.5 bar show that STCS is reduced by about 0.1% only. If we further assume that the available water/brine volume for solubility trapping is not influenced by the presence of impurities in the CO_2 stream, the impact of impurities on solubility storage capacity is defined by

$$\mathrm{STCS} = \frac{M_s}{M_{s_{CO_2}}} = \frac{(\rho_{AqP} X_{CO_2})_{mix}}{\rho_{AqP} X_{CO_2}} \tag{16}$$

where M_s and $M_{s_{CO_2}}$ represent the dissolved mass of CO_2 for impure and for pure CO_2 storage, respectively. In Eq. (16), ρ_{AqP} is the density of brine as a function of temperature, pressure, dissolved gases and brine salinity, is quantified by

$$\rho_s = Mw_{AqP}\left(\frac{x_{H_2O} Mw_{H_2O} + x_{sa} Mw_{sa}}{\rho_0} + \sum_{i=1}^{n} V_i^{Aq} x_i\right)^{-1} \tag{17}$$

where ρ_0 is the pure brine (without dissolved gases) density, computed using a correlation proposed by Rowe and Chou [23] and V^{Aq} is the molar volume of each dissolved component in pure water, calculated from a correlation by Akinfiev and Diamond [24] for various dissolved gases in pure water. The subscript *sa* refers to the salt and the *x*'s are the mole fractions of each component in the aqueous phase which are calculated with the equation of state (EOS) developed by Ziabakhsh-Ganji and Kooi [12]. The EOS describes the thermodynamic equilibrium between a non-aqueous phase (NaqP), basically a multi-component mixture (CO_2, O_2, H_2S, CH_4, Ar, N_2 and SO_2) that can be in gas, supercritical or condensed conditions, and an aqueous phase (AqP), that may include dissolved hydrocarbons and gases in addition to water and dissolved solids and does not include solid/minerals as a separate phase. This EOS predicts the water content in non-aqueous phase and composition of the various gas components in the aqueous and non-aqueous phase at moderate temperatures, a wide pressure range and various salinities (up to 6 mole per kilogram water).

3. Results and discussion

3.1. Support for the applicability of the NaqP model

Fig. 1 illustrates the performance of the model used for the NaqP calculations (for STCV) relative to data in the NISTa [21] database (http://webbook.nist.gov/chemistry/fluid/) for pure (single component) gases. The figure shows that predicted densities compare favorably with the observational data.

For CO_2-mixtures, lack of published experimental density data precludes similar direct validation of the density predictions of our model. In general the validity of density models for mixtures fundamentally depends on the accuracy/validity of the employed binary interaction coefficients (Table 1), which are generally constrained through fitting of experimental data on the vapour liquid equilibrium (VLE) conditions (boundary of the domain in which the two phases co-exist). Li and Yan [17] reported that their binary interaction coefficient for CO_2–SO_2 (0.046) was based on limited VLE data. Therefore, we re-fitted our model to the comprehensive VLE data of Cummings [18]. Fig. 2 shows the fit, and the inferred interaction coefficient (0.047) is listed in Table 1.

Fig. 3 demonstrates that our model predictions for binary mixtures are similar to those of the SUPERTRAPP commercial software [25,26], which methodology is not fully disclosed. Similar agreement was found for other pressures. Although this model–model comparison does not provide formal validation of our model, it does provide confidence that our approach is well suited to evaluate the impact of these impurities on STCV.

Chapoy et al. [27] conducted density measurements on a four-component synthetic gas mixture representative of oxyfuel flue gas containing CO_2, O_2, Ar, and N_2. Fig. 4 shows that our model accurately reproduces these multi-component gas density data.

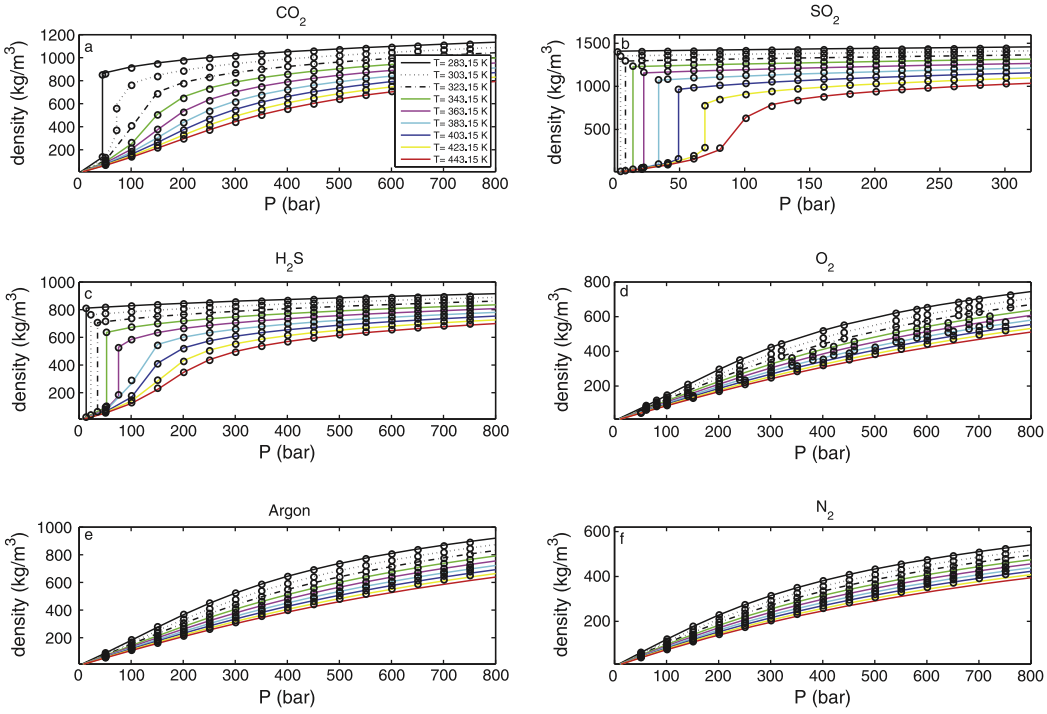

Fig. 1. Density of six component gases considered in this study. Solid lines: this work. Symbols: NISTa [21] database.

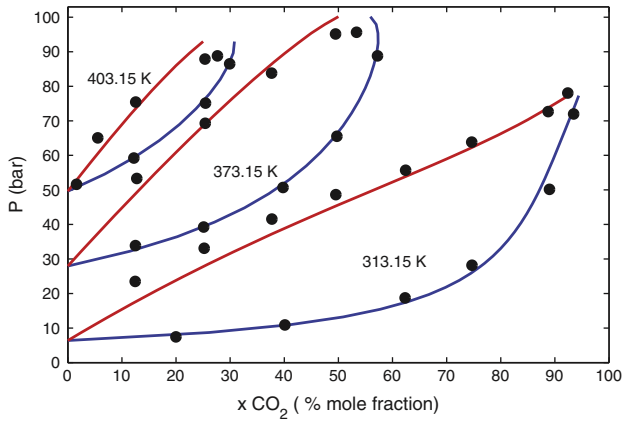

Fig. 2. Comparison of vapour liquid equilibrium (VLE) conditions predicted by the model for a binary mixture of CO_2–SO_2 (solid lines) with experimental data [18] (symbols). Red curves: dew line; blue curves: bubble line. (For interpretation of the references to colour in this figure legend, the reader is referred to the web version of this article.)

3.2. Effect of impurities on the STCV

Fig. 3 illustrates the contrasting influence of the contaminant-gases on mixture density. CH_4, Ar, N_2 and O_2 decrease mixture density, while presence of H_2S, and in particular SO_2 increase mixture density. Note that for ideal gas mixtures, density would progress linearly between the two end-member (pure gases) densities. In that case STCV would equal the CO_2 mole fraction of the mixture and impurities would reduce the CO_2 storage capacity in a trivial way. The nonlinear nature of the curves of Fig. 3 therefore is of particular interest here. The concave nature of the curves of Fig. 3a–d shows that CH_4, Ar, N_2 and O_2 decrease mixture density more strongly than for ideal mixtures and, therefore, have a marked negative impact on the CO_2 storage capacity. For H_2S and SO_2 the impact on volumetric storage capacity is less trivial. A conspicuous and interesting feature of Fig. 3f is that for a CO_2–SO_2 mixture at relatively low temperature density can double for SO_2 mole fraction increases less than 10%. This indicates that CO_2–SO_2 mixtures may occupy a considerably smaller volume than pure CO_2 at the same pressure and temperature conditions. The implications for the CO_2 storage capacity is illustrated in detail below.

Fig. 5 illustrates, for impurity amounts up to 10%, that where other gases decrease STCV, SO_2 can increase the CO_2 storage capacity. Importantly, increased storage occurs within pressure and temperature ranges that are relevant to CCS. Comparison with calculations presented by Wang et al. [11] for 2.9% SO_2 and 330 K shows that our model, which includes density corrections to the PR EOS, yields a higher maximum value (STCV = 1.054 versus STCV = 1.064). Greater impacts than predicted by Wang et al. [10] (more negative STCV values) were also found for oxyfuel flue gas compositions (Table 4).

Fig. 6 (top panels) shows that, for SO_2 mole fractions up to 20%, the maximum CO_2 storage capacity (for fixed temperature and variable pressure or vice versa shown in the panels) increases for increasing amounts of SO_2 in the mixture. The amount of SO_2 also influences the pressure and temperature for which maximum storage capacity occurs. However, the pressure and temperature window for which STC > 1 appears relatively insensitive to the amount of SO_2. The other panels of Fig. 6 illustrates the analogous impacts of other contaminant gases. For Ar, the storage capacity consistently decreases for increasing Ar mole fractions. For H_2S the behavior is more complex; low mole fractions cause a storage capacity decrease, but STCV values > 1 can occur when the H_2S content is very high (e.g., 60% has been reported by [28]).

The different behaviors of the various contaminant gases is controlled primarily by the critical temperature (Tc for SO_2 for instance is very high compared to the other gases) and to a lesser

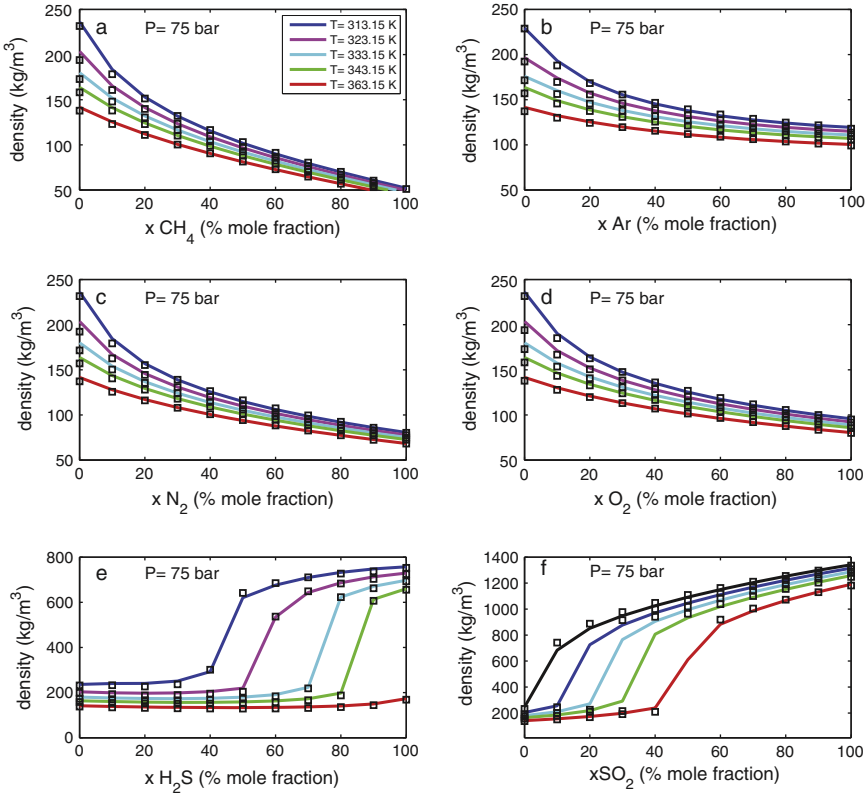

Fig. 3. Density of binary mixtures of CO_2 and an impurity component for the six contaminant gases considered in this study, for 75 bar and various temperatures shown in the legend of (a). Solid lines: this work. Symbols: values obtained using the SUPERTRAPP software [25].

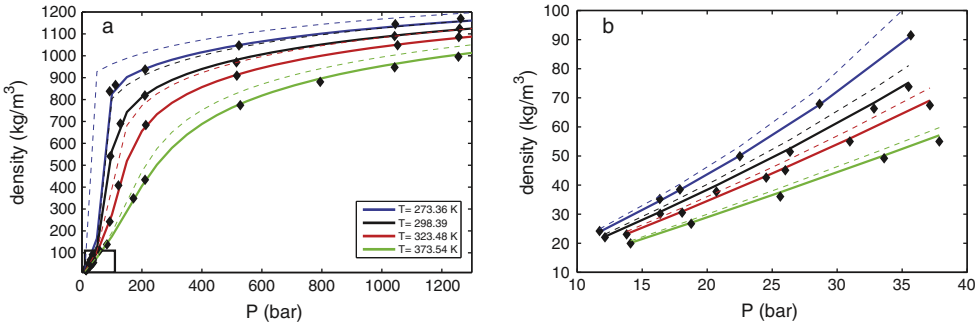

Fig. 4. Density behavior of a four-component gas mixture. Composition (89.83 mol% CO_2, 5.05% O_2, 2.05% Ar, 3.07% N_2) and experimental density data (symbols) from Chapoy et al. [27]. Solid lines: this work. Dashed lines: pure CO_2.

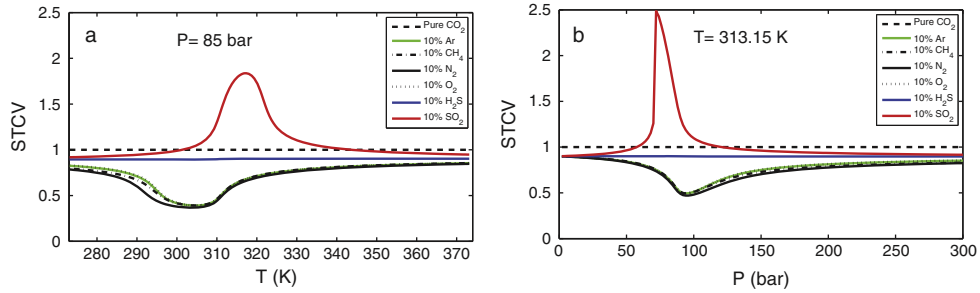

Fig. 5. Calculated STCV for binary gas mixtures containing 10% impurity. (a) Constant temperature. (b) Constant pressure.

Table 3
Typical major components of oxyfuel flue gas [10].

Components	CO_2	O_2	N_2	Ar	Total
Low impurities (moles)	98	0.67	0.74	0.59	100
High impurities (moles)	85	4.73	5.8	4.47	100

extent by the binary interaction coefficient and the critical pressure. Molecular weight does not play a role. This was inferred through simple sensitivity analyses where we recalculated STCV impacts for the various gases while changing one of the above parameters at a time.

Contour plots of the CO_2 storage capacity for CO_2–SO_2 mixtures are presented in Fig. 7 for a wide range of *P*–*T* conditions common in CCS. Results show that the greatest impact of SO_2 occurs at relatively low pressures (74–100 bar) and temperatures (313–325 K). These pressures and temperatures are typical for relatively shallow saline aquifers like, for instance, the Utsira formation (~1 km depth) which is currently used to store CO_2 obtained from the Sleipner gas field in the North Sea. For such storage sites, presence of SO_2 would clearly be favorable. However, Fig. 7 also shows that for deeper aquifers where pressure and temperatures are usually higher (e.g., 180 bar and 340 K at 2 km depth), the CO_2 storage capacity is enhanced only very little or is even reduced due to the presence of SO_2. For depleted oil and gas reservoirs where pore pressures are relatively low, injection of CO_2 at about 80 bar and at low temperatures appears quite realistic, and these conditions can to a large extent be controlled. Therefore, the positive effects of SO_2 on the CO_2 storage capacity can, in principle, also be exploited for storage in depleted hydrocarbon reservoirs. However, following the injection phase in deep reservoirs, the temperature of the stored CO_2-rich gas should be expected to gradually rise to the pre-injection reservoir temperature, which typically is higher than 350 K. Our results show that this warming would be accompanied by expansion of the gas (reduction of STC), which would give rise to a gradual – probably on time scales of thousands of years – post-injection increase of the pore pressure. Although evaluation of the magnitudes of such long-term pressure increases would require further study, they should be of interest for assessments of the long-term reservoir integrity of CCS sites.

Fig. 7c and d shows that for given pressure and temperature conditions an optimum amount of SO_2 exists for which the CO_2 storage capacity is greatest. For increasing temperature this

Table 4
Effect of oxyfuel flue gas[a] on STCV and STCS.

Cases	Depth (m)	*P* (bar)	*T* (K)	Low impurities STCS	High impurities STCS	Low impurities STCV	High impurities STCV	High impurities STCV [10]
Shallow-low temp	895	92	306.15	0.982	0.898	0.902	0.361	0.392
Shallow-mid temp	895	92	311.15	0.980	0.881	0.825	0.389	0.427
Shallow-high temp	895	92	318.15	0.981	0.867	0.873	0.538	0.573
Median-low temp	2336	240	335.15	0.981	0.870	0.961	0.721	0.734
Median-mid temp	2336	240	348.15	0.981	0.868	0.959	0.715	0.731
Median-high temp	2336	240	365.15	0.981	0.865	0.958	0.721	0.739
Deep-low temp	3802	388	365.15	0.981	0.863	0.969	0.776	0.786
Deep-mid temp	3802	388	386.15	0.981	0.862	0.968	0.775	0.787
Deep-high temp	3802	388	414.15	0.981	0.862	0.969	0.782	0.794

[a] Compositions listed in Table 3.

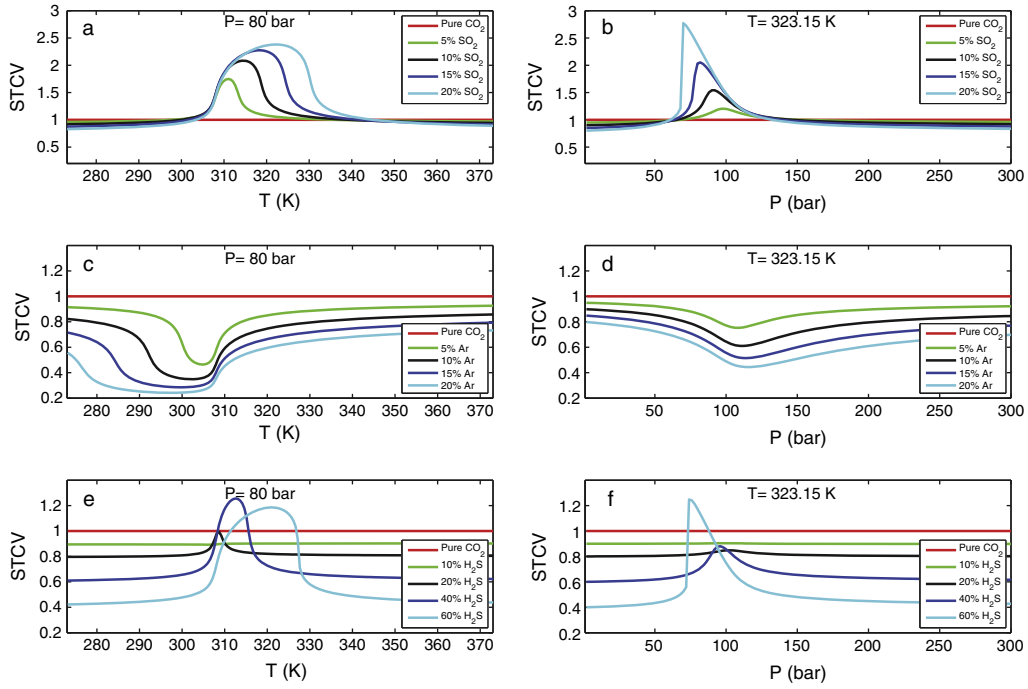

Fig. 6. The impact of the amount of impurity on STCV for various binary gas mixtures. (a and b) CO_2–SO_2. (c and d) CO_2–Ar. (e and f) CO_2–H_2S.

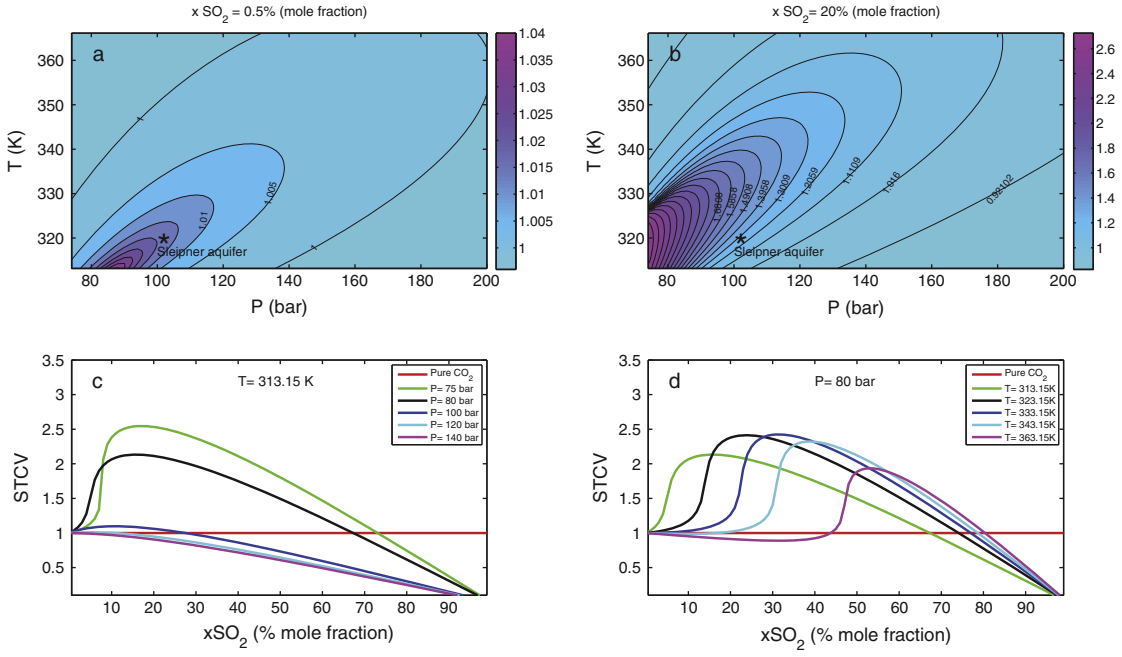

Fig. 7. STCV behavior of SO_2–CO_2 for a wide range of *P*–*T* conditions. (a) 0.5% SO_2 mole fraction, (b) 20% SO_2 mole fraction, (c) variable composition and constant temperature and (d) variable composition and constant pressure.

optimum rapidly becomes exceedingly high. Even for low temperatures the mole fraction of SO_2 required to obtain the greatest positive impact on CO_2 storage is larger than 10%, the feasibility of which is discussed in Section 3.4 below.

3.3. Effect of impurities on STCS

Fig. 8 (panels a and b) shows that presence of N_2 decreases the solubility storage capacity of CO_2, STCS. Decreases of STCS are also predicted for H_2S (panels c and d) and most other gases (Ar, O_2, CH_4). SO_2 again shows deviating behavior; it enhances CO_2 solubility and increases STCS (panels a and b). The STCS enhancement increases with pressure, and (at 100 bar) shows a relatively complex temperature dependency with largest impacts occurring between approximately 320 and 350 K.

As shown in Fig. 9a presence of SO_2 in the CO_2 stream leads to marked density enhancement of the aqueous phase. This is of particular interest for storage in saline aquifers where dissolution of the free gas that has migrated on top of the groundwater can cause an instable density stratification and free convection in the top of the aquifer. The convection continuously moves the layer of saturated water downward, replacing it with unsaturated water,

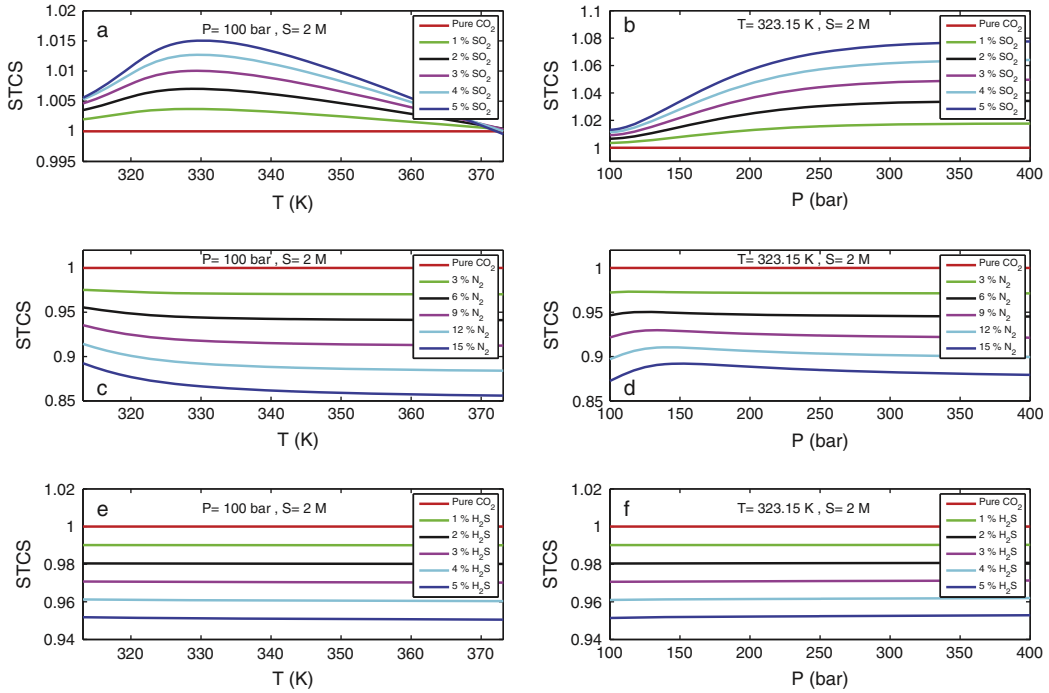

Fig. 8. The impact of the amount of impurity on STCS for various binary gas mixtures. (a and b) CO_2–SO_2. (c and d) CO_2–Ar. (e and f) CO_2–H_2S.

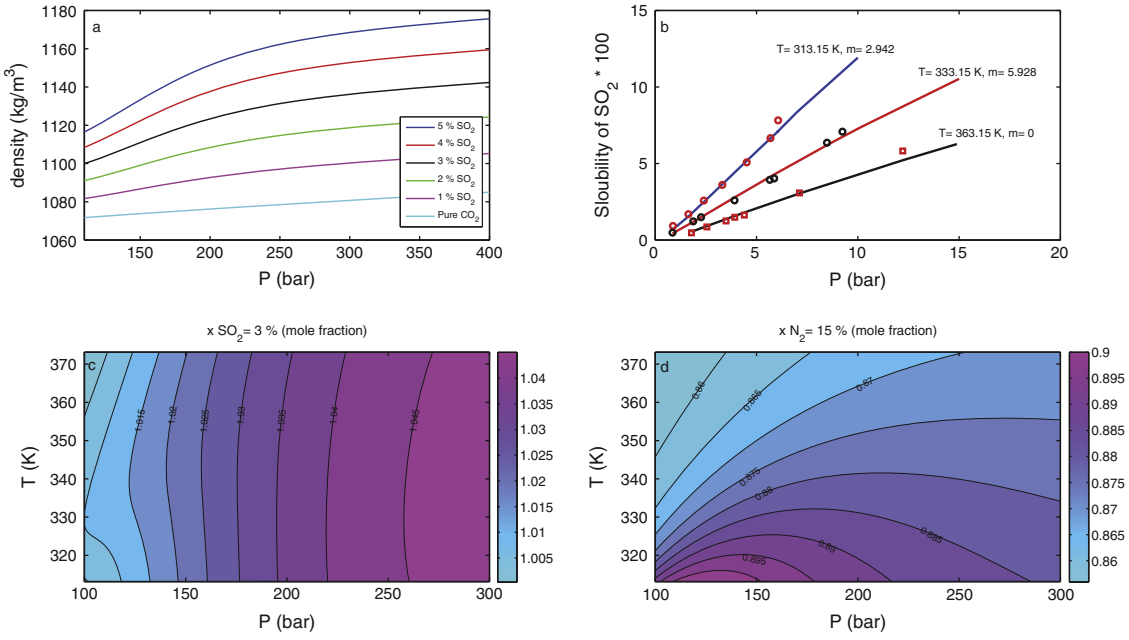

Fig. 9. (a) Solubility of SO_2 for a range of values for temperature, pressure and salinity. Solid line: Ziabakhsh and Kooi's EOS [12]. Symbols: experimental data [39,40]. (b) Aqueous phase density in the presence of SO_2 from the present work. (c) STCS-behavior for a wide range of *P*–*T* conditions of SO_2–CO_2. (d) STCS-behavior for a wide range of *P*–*T* conditions of N_2–CO_2.

thus enhancing the dissolution process [5,29–31]. The results, therefore, suggest that presence of SO_2 not only enhances the ultimate storage of CO_2, but also the dissolution process or dissolution rates.

Fig. 9b shows model-calculated solubility of SO_2 in comparison with available experimental data. Because experimental data are very scarce for SO_2, model predictions are associated with relatively large uncertainty, in particular for pressures beyond about 10 bar. Contour plots of STCS for CO_2–SO_2 mixtures and CO_2–N_2 are presented in Fig. 9c and d for a wide range of *P*–*T* conditions common in CCS. Results show that at pressures beyond 100 bar, the positive impact of SO_2 on CO_2 storage is rather insensitive to temperature. By contrast, the negative impact of N_2 is rather sensitive to both pressure and temperature and least negative effects occur for relatively low pressure and temperature.

Finally, Table 4 lists calculated STCS values for oxyfuel flue gas with low and high impurity contents (compositions shown in Table 3). The chosen values for depth, pressure and temperature

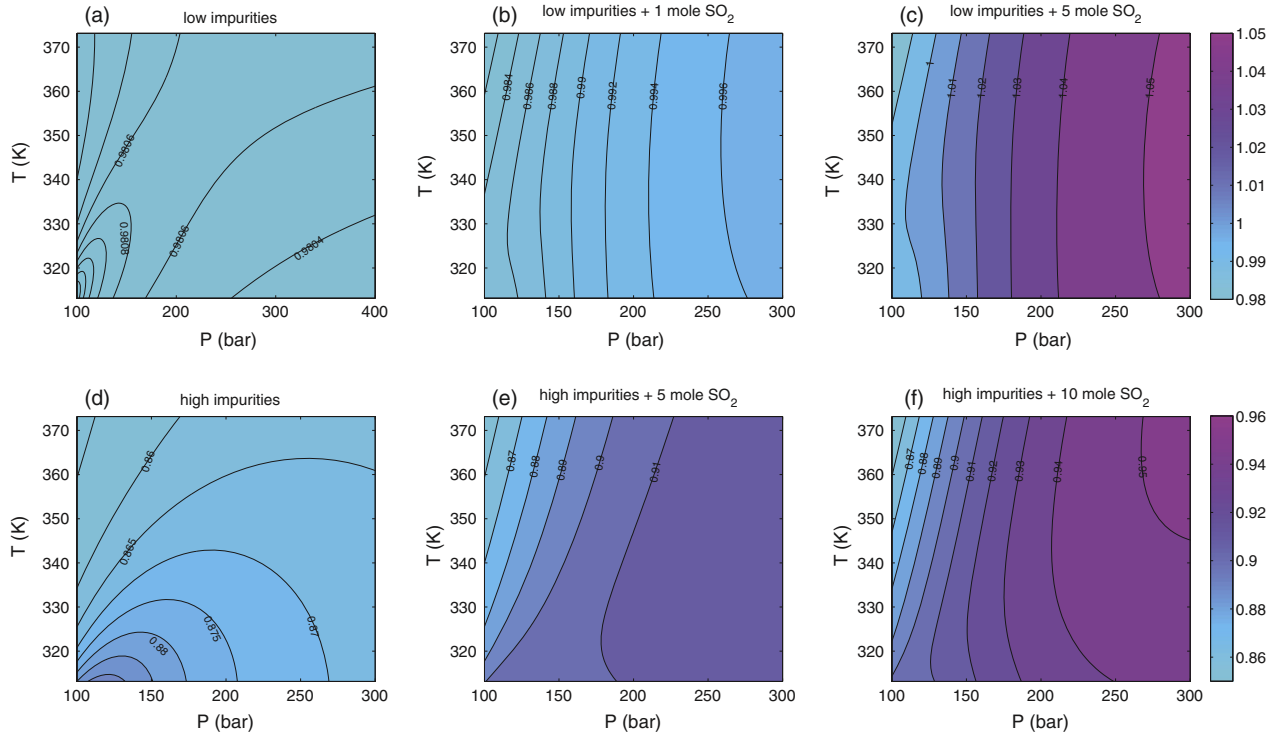

Fig. 10. The impact on STCS of SO_2 addition to oxyfuel flue gas. Top panels: low impurity oxyfuel. Lower panels: high impurity oxyfuel. Oxyfuel compositions are listed in Table 3.

Table 5
Range of mole fractions of impurities in CCS source gases [33].

Component	SO_2	H_2S	CO_2	N_2	O_2	Ar	CH_4
Min mole%	<0.0001	0.01	40 [28]	0.02	0.04	0.005	0.7
Max mole%	2.9 [34]	60 [28]	99	10	5	3.5	4

in Table 4 are representative for the large range of conditions (cases) in saline aquifers that are considered for CO_2 storage, and that have been determined from a global assessment in the framework of the International Energy Agency's Greenhouse Gas Programme (IEA GHG) [32]. The salinity of the saline aquifer has been assumed 2 mol per kilogram water in all cases. Inferred STCS values are about 0.98 for low impurity oxyfuel flue gas and the values is rather insensitive to pressure and temperature conditions. For high-impurity flue gas, values range from about 0.86 to 0.90 where STCS is most strongly affected by aquifer depth/pressure. These dependencies are also apparent in the left panels of Fig. 10(a and d). The other panels of Fig. 10(b, c, e and f) illustrate, as an example, how addition of SO_2 to the oxyfuel flue gas (high and low impurities) can compensate for the negative storage impacts of the dominant O_2, N_2 and Ar co-contaminants for storage capacity in solubility trapping.

3.4. Potential use of the positive effect of SO_2

Reported SO_2 contents of potential CCS source gases usually do not exceed 1.5% mole fraction [33]. IEA GHG [34] reported a very high mole fraction of 2.9% (Table 5), although Wang et al., [11], who used the same value in calculations, also state that values in excess of 0.5%, are considered unlikely and only report values less than 0.005%. Although optimum conditions can therefore not be achieved by using these SO_2 contents directly, the present study does show that the SO_2 can have a positive impact on the CO_2 storage capacity and that it may be worthwhile considering retaining the SO_2 in the gas stream. At coal and oil-fired power plants this might imply considerable savings on the costs of flue gas desulfurization (FGD) by techniques such as scrubbing that are widely used to remove SO_2 due to stringent environmental regulations regarding SO_2 emission. Our model shows that, for a SO_2 content of about 0.5% the STCV enhancement can range up to about 4% (Fig. 7).

Given the large positive effect on CO_2 storage capacity, it may even be an option to utilize SO_2 from other sources to enhance the SO_2 content of CO_2-streams to be stored in subsurface reservoirs, although these amounts would likely have to be less than 0.5% because of the strongly negative health impacts of SO_2 and associated strict requirements imposed in HSE (Health, Safety and Environment) regulations. In spite of such restrictions to practical SO_2 amounts, the results presented (including much higher percentages of SO_2) are still useful and relevant to our general understanding of the impact of this gas. As SO_2 contents of flue gases can be exceedingly low (e.g., Table 5), the possibility of addition of SO_2 before subsurface storage seems particularly interesting for storage in depleted hydrocarbon reservoirs, where presence of SO_2 also suppresses Joule Thomson cooling in the vicinity of the well bore during injection of relatively cold gas, thereby limiting potential clogging problems due to freezing of residual pore water or hydrate formation [20]. In comprehensive assessments, these positive effects of SO_2 would also have to be evaluated relative to potential negative effects such as corrosion of steel well casing [35,36] – this can be greatly suppressed by using dry gas injection –, geochemical reactions in the storage reservoir that may reduce well injectivity due to the strong acidification of the reservoir or aquifer brine [37,38], and health and environmental risks associated with potential leakage of SO_2 from the storage reservoir or from transport and injection facilities. Future work may also have to look into the way in which presence of SO_2 would affect the CO_2 storage potential though its effects on mineral dissolution and mineral trapping, which alter the pore space of storage reservoirs.

4. Conclusion

The present study has assessed sensitivity of CO_2 storage capacity (STC) in both solubility trapping (in the aqueous phase) and volumetric trapping (in the non-aqueous phase) induced by presence of impurities (H_2S, CH_4, O_2, N_2, Ar and SO_2) in the stored CO_2. For both forms of trapping STC is shown to be sensitive to the type(s) of impurity present in the gas stream.

For binary mixtures, presence of SO_2 causes anomalous STC behavior compared with other gas species; while other gases reduce the storage capacity for both solubility trapping (STCS) and volumetric trapping (STCV) of CO_2, SO_2 can increase STC for realistic pressure and temperature conditions. The greatest impact of SO_2 on STCV occurs at relatively low pressures (74–100 bar) and temperatures (313–325 K) that are typical for shallow (<1 km) aquifers, or for deeper depleted hydrocarbon reservoirs during the injection stage. STCS enhancement by SO_2 increases with pressure, and at pressures larger than 100 bar STCS is relatively insensitive to temperature. Presence of SO_2 is also expected to enhance the dissolution process or dissolution rates.

For multi-component impurity mixtures such as oxyfuel flue gas, addition of SO_2 can compensate for the negative impact of other impurities.

In particular for low-temperature injection, co-injection of SO_2 with the CO_2 appears to have clear beneficial CO_2 storing consequences by enhancing STC. However, for the relatively low amounts of SO_2 in flue gases, the beneficial effects are rather small. In comprehensive assessments, these positive effects of SO_2 would have to be evaluated relative to possible negative effects due to induced geochemical reactions, corrosion of steel well casings, and risks associated with potential leakage from the storage reservoir. Allowance of SO_2 in the injected gas may nonetheless represent a viable option to reduce the overall costs of reservoir storage of CO_2 through savings in purification of source gases.

Acknowledgments

This work was made possible by support of the Dutch national research programme CATO2 on CO_2 capture, transport and storage: Work Package 3.2: Reservoir behaviour. Two anonymous reviewers are thanked for their detailed and constructive comments. We would further like to thank Mr. Mohsen Mohammadi for advice regarding constraining the binary interaction coefficient for SO_2.

References

[1] IPCC special report on carbon dioxide capture and storage. Prepared by working group III of the intergovernmental panel on climate change. Cambridge, United Kingdom and New York, NY, USA: Cambridge University Press; 2007.
[2] Kather A. Presented at 2nd working group meeting on CO_2 quality and other relevant issues Cottbus, Germany; 2009.
[3] Kather A, Kownatzki S. Assessment of the different parameters affecting the CO_2 purity from coal fired oxyfuel process. Int J Greenhouse Gas Contr 2011;5(1):S204–9.
[4] IPCC. In: Solomon S, Qin D, Manning M, Chen Z, Marquis M, Averyt KB, Tignor M, Miller HL, editors. Contribution of working group I to the fourth assessment report of the intergovernmental panel on climate change. Cambridge, United Kingdom/New York: Cambridge University Press; 2005.
[5] Bachu S, Bonijoly D, Bradshaw J, Burruss R, Holloway S, Christensen NP, et al. CO_2 storage capacity estimation: methodology and gaps. Int J Green Gas Control 2007;1:430–43.
[6] Tseng CC, Hsieh BZ, Hu ST, Lin ZS. Analytical approach for estimating CO_2 storage capacity of produced gas reservoirs with or without a water drive. Int J Greenhouse Gas Control 2012;9:254–61.
[7] Zhou Q, Birkholzer JT, Tsang CF, Rutqvist J. A method for quick assessment of CO_2 storage capacity in closed and semi-closed saline formations. Int J Green Gas Contr 2008;2:626–39.
[8] Denga H, Stauffer PH, Dai Z, Jiao Z, Surdam RC. Simulation of industrial-scale CO_2 storage: multi-scale heterogeneity and its impacts on storage capacity, injectivity and leakage. Int J Green Gas Contr 2012;10:397–418.
[9] Metz B, Davidson O, de Coninck HC, Loos M, Meyer LA. IPCC special report on carbon dioxide capture and storage. Cambridge, U.K.: Cambridge University Press; 2005.
[10] Wang J, Ryan D, Anthony EJ, Wigston A, Basava-Reddi L, Wildgust N. The effect of impurities in oxyfuel flue gas on CO_2 storage capacity. Int J Greenhouse Gas Contr 2012;11:158–62.
[11] Wang J, Ryan D, Anthony EJ, Wigston A. Effects of impurities on geological storage of carbon dioxide. Report for IEA GHG; 2011.
[12] Ziabakhsh-Ganji Z, Kooi H. An Equation of State for thermodynamic equilibrium of gas mixtures and brines to allow simulation of the effects of impurities in subsurface CO_2 storage. Int J Greenhouse Gas Contr 2012;11S:21–34.
[13] Peng DY, Robinson DB. A new two-constant equation of state. Ind Eng Chem Fundam 1976;15:59–64.
[14] Mathias PM, Naheiri TL, Oh EM. A density correction for the Peng–Robinson Equation of State. Fluid Phase Equilib 1989;47:77–87.
[15] Peneloux A, Rausy E, Freze R. A consistent correction for Redlich–Kwong–Soave volumes. Fluid Phase Equilib 1982;8:7–23.
[16] Prausnitz J, Lichtenthaler M, Gomes RN. Molecular thermodynamics of fluid-phase equilibria. 2nd ed. New York: Prentice Hall; 1986.
[17] Li H, Yan J. Evaluating cubic equations of state for calculation of vapor–liquid equilibrium of CO_2 and CO_2-mixtures for CO_2 capture and storage processes. Appl Energy 2009;86:826–36.
[18] Cummings LWT. High-pressure rectification. I- Vapor-liquid equilibrium relations at high pressures. Ind Eng Chem 1931;23:900–2.
[19] Danesh A. PVT and phase behavior of petroleum reservoir fluids. Elsevier; 1998.
[20] Ziabakhsh-Ganji Z, Kooi H. Sensitivity of Joule-Thomson cooling to impure CO_2 injection in depleted gas reservoirs. Appl Energy 2014;113:434–51.
[21] NISTa. NIST reference fluid thermodynamic and transport properties. Database REFPROP version 7. <http://webbook.nist.gov/chemistry/fluid/>.
[22] Bachu S, Adams JJ. Sequestration of CO_2 in geological media in response to climate change: capacity of deep saline aquifers to sequester CO_2 in solution. Energy Convers Manage 2003;44:3151–75.
[23] Rowe AM, Chou JCS. Pressure–volume–temperature–concentration relation of aqueous NaCl solutions. J Chem Eng Data 1970;15:61–6.
[24] Akinfiev NN, Diamond LW. Thermodynamic description of aqueous nonelectrolytes at infinite dilution over a wide range of state parameters. Geochim Cosmochim Acta 2003;67(4):613–27.
[25] NISTb. Standard reference database 4. NIST thermophysical properties of hydrocarbon mixtures. Program SUPERTRAPP – version 3.2. Gaithersburg, MD 20899, USA; 2007.
[26] Battistelli A, Marcolini M. TMGAS: a new TOUGH2 EOS module for the numerical simulation of gas mixtures injection in geological structures. Int J Greenhouse Gas Contr 2009;3:481–93.
[27] Chapoy A, Nazeri M, Kapateh M, Burgass R, Coquelet C, Tohidi B. Effect of impurities on thermophysical properties and phase behaviour of a CO_2-rich system in CCS. Int J Greenhouse Gas Contr 2013;19:92–100.
[28] ExxonMobil. Carbon capture and sequestration project database. Shute creek treating facility. LaBarge, Wyoming, USA. <https://sequestration.mit.edu/tools/projects/la_barge.html>.
[29] Ennis-King JP, Paterson L. Role of convective mixing in the long-term storage of carbon dioxide in deep saline formations. SPE J 2003;10:349–56.
[30] Li D, Jiang X. A numerical study of the impurity effects of nitrogen and sulfur dioxide on the solubility trapping of carbon dioxide geological storage. Appl Energy 2014;128(1):60–74.
[31] Meybodi HE, Hassanzadeh H. Mixing induced by buoyancy-driven flows in porous media. AIChE J 2013;59:1378–89.
[32] Gorecki CD, Sorensen JA, Bremer JM, Knudsen DJ, Smith SA, Steadman EN, Harju JA. Development of storage coefficients for determining the effective CO_2 storage resource in deep saline formations. SPE-126444-MS; 2009.
[33] Li H, Jakobsen JP, Wilhelmsen Ø, Yan J. PVTxy properties of CO_2 mixtures relevant for CO_2 capture, transport and storage: review of available experimental data and theoretical models. Appl Energy 2011;88:3567–79.
[34] IEA GHG. Impact of impurities on CO_2 capture, transport and storage. Report No. PH4/32; 2004.
[35] Dugstad A, Halseid M, Morland B. Effect of SO_2 and NO_2 on corrosion and solid formation in dense phase CO_2 pipelines. Energy Proc 2013;7:2877–87.
[36] Ruhl AS, Kranzmann A. Investigation of pipeline corrosion in pressurized CO_2 containing impurities. Energy Proc 2013;37:3131–6.
[37] Knauss KG, Johnson JW, Steefel CI. Evaluation of the impact of CO_2, co-contaminant gas, aqueous fluid, and reservoir rock interactions on the geologic sequestration of CO_2. Chem Geol 2005;217:339–50.
[38] Xu T, Apps JA, Pruess K, Yamamoto H. Numerical modeling of injection and mineral trapping of CO_2 with H_2S and SO_2 in a sandstone formation. Chem Geol 2007;242(3):319–46.
[39] Rumpf B, Maurer G. Solubilities of hydrogen cyanide and sulfur dioxide in water at temperatures from 293.15 to 413.15 K and pressures up to 2.5 MPa. Fluid Phase Equilib 1992;81:241–60.
[40] Xia J, Rumpf B, Maurer G. The solubility of Sulfur dioxide in aqueous solutions of sodium chloride and ammonium chloride in the temperature range from 313 K to 393 K at pressures up to 3.7 MPa: experimental results and comparison with correlations. Fluid Phase Equilib 1999;165:99–119.